

Nonsteroidal Anti-Inflammatory Drugs–1-Phenylethylamine  
Diastereomeric Salts: A Systematic Solid-State Investigation

Patrizia Rossi, Jacopo Ceccarelli, Stella Milazzo, Paola Paoli,\* Juliana Morais Missina, Samuele Ciattini, Andrea Ienco, Giulia Tuci, Maurizio Valleri, Maria Paola Giovannoni, Gabriella Guerrini, and Luca Conti

Cite This: *Cryst. Growth Des.* 2021, 21, 6947–6960

Read Online

ACCESS |



Metrics &amp; More

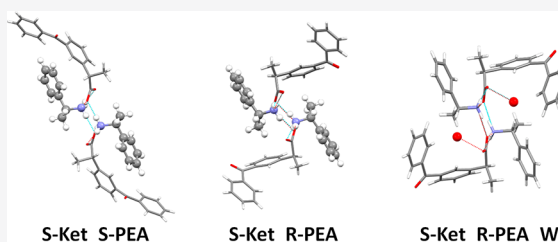


Article Recommendations



Supporting Information

**ABSTRACT:** The solid-state investigation of the diastereomeric salts (S)-ibuprofen (S-Ibu), (S)-naproxen (S-Nap), and (S)-ketoprofen (S-Ket) with (R)-(+)- and (S)-(–)-1-phenylethylamine, R-PEA, and S-PEA respectively, has been carried out by using a combination of experimental and *in-silico* tools. The focus was on their crystal packing and on the stability/transformation of their solid forms under different experimental conditions with the final aim of extracting useful information on the forces/features which could be exploited for the chiral separation of the corresponding racemic compounds. All the salts are 2<sub>1</sub>-column crystals, each column consisting of API and 1-phenylethylamine ions assembled via the 1-phenylethylammonium-carboxylate supramolecular heterosynthon which originates a R<sub>4</sub><sup>3</sup> (10) pattern, the intercolumns contacts being definitely weaker. In spite of an overall similarity in the crystal packing forces and motifs of the anhydrous salts, the temperature stability range suggests that the homochiral species are the most stable. The fact that the homochiral salt of S-Ket (S-Ket\_S-PEA) is stable toward the hydration, at variance with the heterochiral one (S-Ket\_R-PEA), further confirms this hypothesis. On the other hand, preliminary sorption tests show that S-Ket and S-Ibu preferentially capture the homochiral PEA (S-Nap is not selective). This behavior has been correlated to the almost planar boundary surfaces which characterize and differentiate the 2<sub>1</sub> sheets in S-Ket\_S-PEA and S-Ibu\_S-PEA salts with respect to the corresponding heterochiral ones.

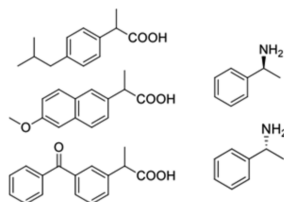


## INTRODUCTION

Nonsteroidal anti-inflammatory drugs (NSAIDs) are widely used to reduce pain and inflammation. Among the many NSAIDs available, there are ibuprofen ((RS)-2-(4-isobutylphenyl)propanoic acid), naproxen ((RS)-2-(6-methoxy-2-naphthyl)propanoic acid), and ketoprofen ((RS)-2-(3-benzoylphenyl)propanoic acid), all belonging to the class of arylpropionic acid derivatives (Scheme 1). They are BCS class II drugs<sup>1</sup> (i.e., they are characterized by high permeability and low solubility), and because of their poor aqueous solubility, they are usually formulated as inorganic (e.g., ibuprofen, naproxen, and ketoprofen as sodium salts) as well as organic

salts (ibuprofen as arginine or lysine salts; ketoprofen as a lysine one). Moreover, given the presence of one stereogenic center (the  $\alpha$ -carbon of propionic acid), they exist as a pair of enantiomers, and although only the S one is the active pharmaceutical ingredient (API),<sup>2</sup> they are usually administered as racemic mixtures. However, over the last few years, interest in single-enantiomer formulations has increased due to several clinical advantages, including easier/improved pharmacokinetic and pharmacodynamic profiles, lower prescribed amount, and reduced toxicity, just to name a few.<sup>3</sup> The development of a single-enantiomer drug starting from the corresponding chiral one, previously developed as a racemic mixture, is referred to as a “chiral switch”. The change in the status of the drug chirality, i.e., the chiral switch, also implies patent issues, e.g., enantiomer patents, a kind of secondary pharmaceutical patent, which claims a single enantiomer of a chiral drug previously claimed as a racemate.<sup>4,5</sup> Ibuprofen was the first NSAID to be switched to the single-enantiomer

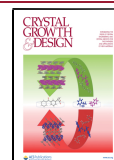
**Scheme 1.** Left: Schematic Drawing of Ibuprofen (Top), Naproxen (Middle) and Ketoprofen (Bottom) and Right: (S)-(–)-1-Phenylethylamine (Top) and (R)-(+)-1-Phenylethylamine (Bottom)



Received: August 4, 2021

Revised: September 23, 2021

Published: November 4, 2021



formulation,<sup>6</sup> followed by ketoprofen four years later (1998),<sup>7</sup> and their S enantiomers are also marketed in several fixed-dose combination drugs, as well as (S)-naproxen.

Enantiopure APIs may be obtained via asymmetric syntheses (usually expensive and time-consuming) or via separation of the two isomers, for example, through chromatographic resolution, enzymatic resolution, or formation of diastereomeric salts (DSs).<sup>8,9</sup> Classical racemic resolution via DSs formation, which exploits their different physicochemical properties (e.g., melting point, solubility) for the separation, involves a racemic chiral acid (base) and a basic (acid) optically active resolving agent. Low cost coupled with the recovery of the resolving agent are the usual advantages of this widely used method in the pharmaceutical industry. By contrast, the selection of the best resolving agent as well as the best experimental conditions is usually time-consuming and largely empirical. Studies on structurally related diastereomeric salts<sup>10</sup> can help to overcome this trial-and-error approach providing useful hints for the resolving agent choice. In this context, in-depth and systematic investigations of the solid forms of strictly related diastereomeric salts could provide useful suggestions about the forces/features to be exploited for successful resolutions.

In the past, we have used X-ray diffraction (SCXRD, PXRD) thermoanalytical techniques (DSC, TGA, and HSM) and *in-silico* tools (e.g., modeling and data mining) to study the solid forms of APIs belonging to different classes ( $\beta$ -blockers,<sup>11,12</sup> NSAIDs) and in different forms (salts<sup>13–15</sup> and metal complexes)<sup>16</sup> and to correlate their structural and physicochemical properties.<sup>17,18</sup>

With this in mind, and as part of our ongoing structural study of (S)-ketoprofen (S-Ket, hereafter),<sup>19–21</sup> its DSs with (R)-(+)- and (S)-(–)-1-phenylethylamine ( $\alpha$ -methylbenzylamine; R-PEA and S-PEA, hereafter, Scheme 1) were prepared and investigated. 1-Phenylethylamine was chosen because (1) it is a commonly used resolving agent (it is cheap, and it has the chiral center close to the functional group involved in the recognition event); (2) with carboxylic acids, it forms robust charge-assisted hydrogen-bonded heterosynthons;<sup>22</sup> (3) the structures of both the homochiral and heterochiral DSs with (S)-ibuprofen (S-Ibu, hereafter) have already been described<sup>23,24</sup> as well as that of (S)-naproxen (S-Nap, hereafter) with R-PEA,<sup>25</sup> thus providing a first set of closely structurally related diastereomeric salts.

The set of investigated salts was completed by adding the S-Nap\_S-PEA salt. During the solid-state investigation of S-Ket\_R-PEA, a partially hydrated species was identified. Finally, given that we were also interested in studying the DSs in bulk, fresh samples of S-Ibu\_S-PEA, S-Ibu\_R-PEA, and S-Nap\_R-PEA were prepared.

In summary, we herein present the results of the experimental and *in-silico* investigation of the solid forms of the seven structurally related DSs of S-Ket, S-Ibu, and S-Nap with R- and S-PEA, including the partially hydrated species of S-Ket\_R-PEA (S-Ket\_R-PEA\_W, hereafter). Their crystal structures have been discussed and compared to each other, and their bulk properties in terms of thermal and phase stabilities (including hydration/dehydration processes) have been assessed. Similarities and differences have been evidenced and correlated with NSAIDs selective PEA-sorption propensities with the final aim of extracting useful information about the factors governing the chiral separation of their corresponding racemic compounds.

## EXPERIMENTAL SECTION

**Chemicals.** (S)-(+)-2-(6-Methoxy-2-naphthyl)propionic acid ((S)-(+)-naproxen, 99%) was purchased from Alfa Aesar. (S)-(+)-Ibuprofen (98%), (S)-(+)-ketoprofen (99%), (S)-(–)-1-phenylethylamine (99%), and (R)-(+)-1-phenylethylamine (99%) were purchased from Sigma-Aldrich. All of the APIs were used without further purification.

**Procedures for Salt Preparation.** All syntheses were carried out in air at room temperature (rt) using ultrapure water (Milli-Q, Millipore type 1, 18.2 M $\Omega$  cm resistivity at 25 °C) and ethanol (96%) purchased from Sigma-Aldrich, used without further purification. Preliminary melting points of the prepared salts were measured on a Stuart Scientific SIMP3 apparatus and are uncorrected. <sup>1</sup>H NMR spectra were recorded with a Varian Mercuryplus 400 instrument, operating at 400 MHz.

To make sure that each microcrystalline powder sample contained the same phase as the corresponding single crystals, its rt PXRD pattern was compared with the theoretical one obtained from SCXRD data (see Figures S1–S7).

**Synthesis of (S)-(–)-1-Phenylethylammonium (S)-(+)-2-(4-Isobutylphenyl)propionate (S-Ibu\_S-PEA) and (R)-(+)-1-Phenylethylammonium (S)-(–)-2-(4-Isobutylphenyl)propionate (S-Ibu\_R-PEA).** Both (S)-(+)-ibuprofen (206.3 mg, 1 mmol) and (S)-(–)-1-phenylethylamine or (R)-(+)-1-phenylethylamine (129  $\mu$ L, 1.0 mmol) were dissolved in 6 mL of a 67% ethanol/water mixture by heating at 60 °C for a minute under magnetic stirring. The solution was cooled to rt, and some of the solvent was allowed to evaporate. After 24 h, the formation of colorless needles was observed. The suspension was filtered to recover the salts. <sup>1</sup>H NMR (methanol-*d*<sub>6</sub>) spectra were collected on the solid products to verify the stoichiometric ratio (1:1) of the salt and to exclude the excess of unreacted starting material. The signals considered were the quartets at ca. 3.60 ppm for ibuprofen and ca. 4.30 ppm for PEA (see Figures S8 and S9).

Yield: 216 mg (66% based on the formula [C<sub>8</sub>H<sub>12</sub>N][C<sub>13</sub>H<sub>17</sub>O<sub>2</sub>] (S-Ibu\_S-PEA) and 190 mg (58% based on the formula [C<sub>8</sub>H<sub>12</sub>N][C<sub>13</sub>H<sub>17</sub>O<sub>2</sub>] (S-Ibu\_R-PEA).

**Synthesis of (S)-(–)-1-Phenylethylammonium (S)-(+)-2-(6-methoxy-2-naphthyl)propionate (S-Nap\_S-PEA) and (R)-(+)-1-Phenylethylammonium (S)-(+)-2-(6-Methoxy-2-naphthyl)propionate (S-Nap\_R-PEA).** Both (S)-(+)-naproxen (230.3 mg, 1 mmol) and (S)-(–)-1-phenylethylamine or (R)-(+)-1-phenylethylamine (129  $\mu$ L, 1.0 mmol) were solubilized together under magnetic stirring in 15 mL of a 70% ethanol/water mixture. Stirring was ceased upon observing the complete dissolution of both reagents, the system was stored at rt, and the vial was sealed with punctured Parafilm. The salts were obtained as colorless needles after partial solvent evaporation at rt for 7 days.

Yield: 221 mg (63% based on the formula [C<sub>8</sub>H<sub>12</sub>N][C<sub>14</sub>H<sub>13</sub>O<sub>3</sub>] (S-Nap\_S-PEA) and 214 mg (61% based on the formula [C<sub>8</sub>H<sub>12</sub>N][C<sub>14</sub>H<sub>13</sub>O<sub>3</sub>] (S-Nap\_R-PEA).

As an alternative method, the reactants were dissolved in ethanol (8 mL) by heating at 60 °C for a minute under magnetic stirring. Then 2 mL of H<sub>2</sub>O was added, and the solution was cooled to rt. After partial evaporation of the solvent, 24 h later, the formation of colorless needles was observed. The suspension was filtered to recover the salts. In all cases, <sup>1</sup>H NMR (methanol-*d*<sub>6</sub>) spectra were collected on the solid products to verify the stoichiometric ratio (1:1) of the salt and to exclude the excess of unreacted starting material. The signals considered were the quartets at ca. 3.60 ppm for naproxen and ca. 4.30 ppm for PEA (see Figures S10 and S11).

Yield: 208 mg (59% based on the formula [C<sub>8</sub>H<sub>12</sub>N][C<sub>14</sub>H<sub>13</sub>O<sub>3</sub>] (S-Nap\_S-PEA) and 239 mg (68% based on the formula [C<sub>8</sub>H<sub>12</sub>N][C<sub>14</sub>H<sub>13</sub>O<sub>3</sub>] (S-Nap\_R-PEA).

**Synthesis of (S)-(–)-1-Phenylethylammonium (2S)-2-(3-Benzoylphenyl)propionate (S-Ket\_S-PEA) and (R)-(+)-1-Phenylethylammonium (2S)-2-(3-Benzoylphenyl)propionate (S-Ket\_R-PEA).** Both (S)-(+)-ketoprofen (254.3 mg, 1.0 mmol) and (S)-(–)-1-phenylethylamine or (R)-(+)-1-phenylethylamine (134  $\mu$ L, 1.05 mmol) were solubilized together under magnetic stirring in 5 mL of a 70%

**Table 1.** Crystal Data and Refinement Parameters of S-Ibu\_S-PEA, S-Nap\_S-PEA, S-Nap\_R-PEA, S-Ket\_S-PEA, S-Ket\_R-PEA, and S-Ket\_R-PEA\_W

	S-Ibu_S-PEA	S-Nap_S-PEA	S-Nap_R-PEA
formula	[C <sub>8</sub> H <sub>12</sub> N][C <sub>13</sub> H <sub>17</sub> O <sub>2</sub> ]	[C <sub>8</sub> H <sub>12</sub> N][C <sub>14</sub> H <sub>13</sub> O <sub>3</sub> ]	[C <sub>8</sub> H <sub>12</sub> N][C <sub>14</sub> H <sub>13</sub> O <sub>3</sub> ]
MW	327.45	351.42	351.42
T (K)	100	100	100
$\lambda$ (Å)	1.54178	1.54178	1.54178
crystal system, space group	orthorhombic, <i>P</i> 2 <sub>1</sub> 2 <sub>1</sub> 2 <sub>1</sub>	monoclinic, <i>P</i> 2 <sub>1</sub>	monoclinic, <i>P</i> 2 <sub>1</sub>
unit cell dimensions (Å, °)	<i>a</i> = 5.8472(1) <i>b</i> = 15.2007(3) <i>c</i> = 22.2281(4)	<i>a</i> = 12.5323(3) <i>b</i> = 5.9648(2); $\beta$ = 102.922(1) <i>c</i> = 13.1780(3)	<i>a</i> = 11.5926(4) <i>b</i> = 5.8932(4); $\beta$ = 94.487(2) <i>c</i> = 13.5680(4)
volume (Å <sup>3</sup> )	1975.67(6)	960.14(5)	924.09(5)
Z, dc (g/cm <sup>3</sup> )	4, 1.101	2, 1.216	2, 1.263
$\mu$ (mm <sup>-1</sup> )	0.544	0.641	0.666
<i>F</i> (000)	712	376	376
crystal size (mm)	0.15 × 0.18 × 0.24	0.14 × 0.15 × 0.19	0.14 × 0.16 × 0.19
reflns collected/unique ( <i>R</i> <sub>int</sub> )	10588/3456 (0.0615)	21660/3404 (0.0669)	13442/3534 (0.0834)
2 $\theta$ range (deg)	7.95/133.62	6.88/136.73	6.53/145.39
data/parameters	3456/304	3404/310	3534/310
final <i>R</i> indices [ <i>I</i> > 2 $\sigma$ ]	<i>R</i> <sub>1</sub> = 0.0463, <i>wR</i> <sub>2</sub> = 0.1183	<i>R</i> <sub>1</sub> = 0.0514, <i>wR</i> <sub>2</sub> = 0.1321	<i>R</i> <sub>1</sub> = 0.0459, <i>wR</i> <sub>2</sub> = 0.1001
<i>R</i> indices (all data)	<i>R</i> <sub>1</sub> = 0.0512, <i>wR</i> <sub>2</sub> = 0.1275	<i>R</i> <sub>1</sub> = 0.0518, <i>wR</i> <sub>2</sub> = 0.1332	<i>R</i> <sub>1</sub> = 0.0550, <i>wR</i> <sub>2</sub> = 0.1063
GOF	1.054	1.108	1.079
	S-Ket_S-PEA	S-Ket_R-PEA	S-Ket_R-PEA_W
formula	[C <sub>8</sub> H <sub>12</sub> N][C <sub>16</sub> H <sub>13</sub> O <sub>3</sub> ]	[C <sub>8</sub> H <sub>12</sub> N][C <sub>16</sub> H <sub>13</sub> O <sub>3</sub> ]	[C <sub>8</sub> H <sub>12</sub> N][C <sub>16</sub> H <sub>13</sub> O <sub>3</sub> ].0.15H <sub>2</sub> O
MW	375.44	375.44	379.75
T (K)	100	100	100
$\lambda$ (Å)	1.54178	1.54178	1.54178
crystal system, space group	orthorhombic, <i>P</i> 2 <sub>1</sub> 2 <sub>1</sub> 2 <sub>1</sub>	orthorhombic, <i>P</i> 2 <sub>1</sub> 2 <sub>1</sub> 2 <sub>1</sub>	monoclinic, <i>P</i> 2 <sub>1</sub>
unit cell dimensions (Å, °)	<i>a</i> = 6.045(2) <i>b</i> = 12.894(4) <i>c</i> = 25.868(9)	<i>a</i> = 6.5660(3) <i>b</i> = 10.2179(5) <i>c</i> = 30.331(1)	<i>a</i> = 12.554(2) <i>b</i> = 6.6768(9); $\beta$ = 93.563(5) <i>c</i> = 12.638(2)
volume (Å <sup>3</sup> )	2030(1)	2034.9(2)	1057.3(3)
Z, dc (g/cm <sup>3</sup> )	4, 1.229	4, 1.225	2, 1.193
$\mu$ (mm <sup>-1</sup> )	0.642	0.641	0.631
<i>F</i> (000)	800	800	405
crystal size (mm)	0.13 × 0.15 × 0.18	0.16 × 0.20 × 0.25	0.14 × 0.18 × 0.22
reflns collected/unique ( <i>R</i> <sub>int</sub> )	17011/4020 (0.0802)	18351/3522 (0.0800)	12599/4091 (0.0755)
2 $\theta$ range (deg)	6.83/149.11	5.83/134.47	7.01/144.84
data/parameters	4020/328	3522/328	4091/337
final <i>R</i> indices [ <i>I</i> > 2 $\sigma$ ]	<i>R</i> <sub>1</sub> = 0.0786, <i>wR</i> <sub>2</sub> = 0.1757	<i>R</i> <sub>1</sub> = 0.0526, <i>wR</i> <sub>2</sub> = 0.1494	<i>R</i> <sub>1</sub> = 0.0519, <i>wR</i> <sub>2</sub> = 0.1307
<i>R</i> indices (all data)	<i>R</i> <sub>1</sub> = 0.0906, <i>wR</i> <sub>2</sub> = 0.1835	<i>R</i> <sub>1</sub> = 0.0596, <i>wR</i> <sub>2</sub> = 0.1602	<i>R</i> <sub>1</sub> = 0.0573, <i>wR</i> <sub>2</sub> = 0.1379
GOF	1.178	1.061	1.083

ethanol/water mixture. Stirring was ceased upon observing the complete dissolution of both reagents, and the system was stored at rt. Colorless needles of the salts formed once the solvent evaporated completely. <sup>1</sup>H NMR (methanol-*d*<sub>6</sub>) spectra were collected on the solid products to verify the stoichiometric ratio (1:1) of the salt and to exclude the excess of unreacted starting material. The signals considered were the quartets at ca. 3.60 ppm for ketoprofen and ca. 4.30 ppm for PEA (see Figures S12 and S13).

**Synthesis of (R)-(+)-1-Phenylethylammonium (2S)-2-(3-Benzoyl-phenyl) Propionate Hydrate (S-Ket\_R-PEA\_W).** Both (S)-(+)-ketoprofen (254.3 mg, 1 mmol) and (R)-(+)-1-phenylethylamine (129  $\mu$ L, 1.0 mmol) were dissolved in 5 mL of a 70% ethanol/water mixture under magnetic stirring. After 5 days, by slow and not complete solvent evaporation, the formation of colorless platelet crystals was observed. <sup>1</sup>H NMR (methanol-*d*<sub>6</sub>) spectra were collected on the solid products to verify the stoichiometric ratio (1:1) of the salt and to exclude the excess of unreacted starting material. The signals considered were the quartets at ca. 3.60 ppm for ketoprofen and ca. 4.30 ppm for PEA (see Figure S14).

Yield: 272 mg (72% based on the formula [C<sub>8</sub>H<sub>12</sub>N][C<sub>16</sub>H<sub>13</sub>O<sub>3</sub>].0.15H<sub>2</sub>O (S-Ket\_R-PEA\_W).

**Single-Crystal X-ray Diffraction.** Single-crystal X-ray diffraction data of S-Ibu\_S-PEA, S-Nap\_S-PEA, S-Nap\_R-PEA, S-Ket\_S-PEA, S-Ket\_R-PEA, and S-Ket\_R-PEA\_W were collected on a Bruker APEX-II CCD diffractometer using Cu-K $\alpha$  radiation. All measurements were performed at 100 K. For compounds S-Ibu\_S-PEA and S-Nap\_R-PEA, this was a redetermination at a lower temperature of already known structures (VAKVEK<sup>24</sup> (173 K) and HIFRIX<sup>25</sup> (rt), respectively).

Diffraction data were collected with the Bruker APEX2 program<sup>26</sup> and reduced with the Bruker SAINT<sup>27</sup> one. Structures were solved using the SIR-2004 package<sup>28</sup> and refined by full-matrix least-squares against *F*<sup>2</sup> using all data (SHELX2018/3.<sup>29</sup> In all structures, the non-hydrogen atoms were anisotropically refined. All hydrogen atoms were found in the Fourier difference map. Their coordinates were freely refined, while their thermal parameters were set in accordance with the atoms to which they are bonded. The occupancy factor of the oxygen water molecule in S-Ket\_R-PEA\_W was set to 0.15 (hydrogen atoms were not added); this value was obtained after several refinement cycles during which it was freely refined.<sup>30</sup> Table 1 reports crystal data and refinement parameters for all structures. In Figure 1, ball and stick views of the asymmetric units of the S-Nap\_S-



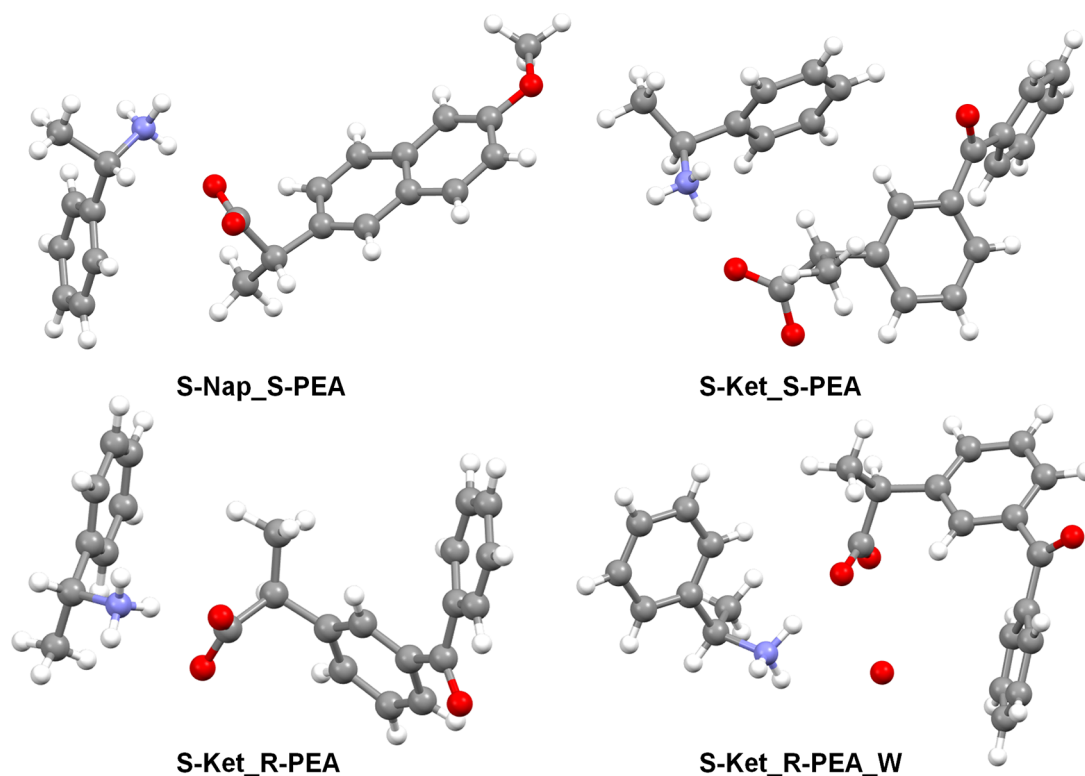


**Figure 1.** Ball and stick view of the asymmetric units of S-Nap\_S-PEA, S-Ket\_S-PEA, S-Ket\_R-PEA, and S-Ket\_R-PEA\_W.

PEA, S-Ket\_S-PEA, S-Ket\_R-PEA, and S-Ket\_R-PEA\_W structures are reported, while the ORTEP-3 view of the asymmetric unit of the above-mentioned four compounds and of S-Ibu\_S-PEA and S-Nap\_R-PEA (all with the atom labels) are in the [Supporting Information](#) (Figures S15–S20). Cell parameters were also determined at 300 K for all the anhydrous salts reported above, plus the already known S-Ibu\_R-PEA salt (CSD Refcode = VUCHOR<sup>23</sup>). For S-Ket\_R-PEA\_W, cell parameters were determined at different temperatures in the 100–340 K range.

**Powder X-ray Diffraction (PXRD).** Room-temperature PXRD measurements were carried out by using a Bruker New D8 Da Vinci diffractometer (Cu–K $\alpha$ 1 radiation = 1.54056 Å, 40 kV  $\times$  40 mA), equipped with a Bruker LYNXEYE-XE detector, scanning range  $2\theta$  = 3–40°, 0.03° increments of  $2\theta$  and counting time of 0.8 s/step. Variable-temperature PXRD analyses of S-Nap\_S-PEA, S-Nap\_R-PEA, and S-Ket\_R-PEA\_W were performed by using an Anton Paar HTK 1200N hot chamber mounted on a Panalytical X'Pert PRO automated diffractometer (Cu–K $\alpha$  radiation, 40 kV  $\times$  40 mA), equipped with a PIX-CEL solid-state fast detector. The scanning range was  $2\theta$  = 5–40° with a 1 s/step counting time and 0.03° increments of  $2\theta$ . The temperature variation rate was 5 K/min. After the target temperature was reached, the sample was kept at that temperature for 5 min before proceeding with data collection. Measures were performed in air.

**Differential Scanning Calorimetry (DSC) and Thermogravimetric Analysis (TGA).** Differential scanning calorimetry (DSC) experiments were performed by using a Mettler Toledo DSC1 Excellence instrument. Measurements were run in aluminum pans with pinhole lids (the samples' mass ranged from 0.8 to 3.2 mg). Temperature and enthalpy calibrations were done using indium as a standard. Measurements were carried out in the 300–490 K range for the S-Ibu and S-Nap salts and in the 300–450 K range for the S-Ket ones. A linear heating rate of 10 K/min was used. Experiments were performed in air. DSC peaks were analyzed using the STARe software.<sup>31</sup> The reported data were the average of two measurements, and standard errors were  $\pm 0.1$  K for temperature and  $\pm 0.3$  kJ/mol for enthalpy.

For the thermogravimetric analyses (TGA), samples were analyzed on an EXSTAR Seiko 6200 analyzer under air (100 mL/min) at a heating rate of 5 K/min from 313 to 873 K. The weight of the samples was between 3 and 5 mg.

**Hydration and Dehydration Tests on (S)-Ketoprofen Salts.** The possible anhydrous  $\rightarrow$  hydrate transformation of S-Ket\_S-PEA and S-Ket\_R-PEA was investigated by keeping the salts in a desiccator at constant relative humidity (ca. 75% by using a saturated solution of NaCl) for a week. At the end of this period, PXRD patterns were collected and compared with those taken at the beginning of the experiment.

In addition, the dehydration process of the S-Ket\_R-PEA\_W salt was investigated by putting the salt in a desiccator for a week with KOH. Then, the PXRD patterns collected at the beginning and at the end of the experiment were compared. Variable-temperature XRD measures were also carried out to check the possibility of triggering the dehydration process by temperature: cell parameters of the S-Ket\_R-PEA\_W salt were determined in the 100–340 K range by SCXRD, and a VT-PXRD experiment was carried out in the 300–390 K range (see the powder X-ray diffraction, PXRD section). Results were then compared with those from TGA and DSC analyses.

**Sorption Tests of *rac*-PEA on (S)-NSAIDs.** In a desiccator, (S)-NSAID (1 mmol) and *rac*-1-phenylethylamine (387  $\mu$ L, 3.0 mmol) were put in two different Petri dishes. The desiccator was kept under a vacuum for 6 days; after that time, a PXRD pattern of the solid originally containing the (S)-NSAID sample was collected. The procedure was repeated for all the S-NSAIDs under investigation.

**Preliminary Thermal Stability Tests on (S)-NSAID Salts.** Each (S)-NSAID salt was kept in an oven for 2 h. The temperature was set about 30 K lower than the melting temperature of the corresponding salt as measured with a Stuart Scientific apparatus: S-Ibu\_S-PEA,  $T$  = 420 K; S-Ibu\_R-PEA,  $T$  = 400 K; S-Nap\_S-PEA,  $T$  = 415 K; S-Nap\_R-PEA,  $T$  = 400 K; S-Ket\_S-PEA,  $T$  = 370 K; S-Ket\_R-PEA,  $T$  = 360 K; S-Ket\_R-PEA\_W,  $T$  = 360 K.

Then, a PXRD pattern of each sample at the end of the experiment was collected and analyzed. Finally, <sup>1</sup>H NMR (CDCl<sub>3</sub>) spectra were collected, and the ratio of NSAID/PEA was evaluated by integration

of the signals. In particular, the quartets at ca. 3.60 and ca. 4.30 ppm were used for NSAID and PEA, respectively.

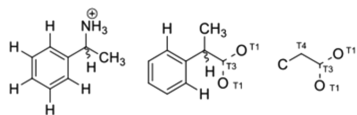
**In-Silico Analysis.** The crystal packing of the seven salts was analyzed with Mercury.<sup>32</sup> Crystal-Explorer17<sup>33</sup> was used to compute the Hirshfeld surfaces (HS) and their associated 2D fingerprint plots in order to further investigate the intermolecular interactions which hold together the crystal of the six anhydrous diastereomeric salts (the S-Ket\_R-PEA\_W, due to the fractional occupancy factor of the crystallization water molecule, was not analyzed).

In addition, a series of solid-state calculations were run on the anhydrous and hydrated salts of S-Ket\_R-PEA. The crystallographic coordinates of S-Ket\_R-PEA and S-Ket\_R-PEA\_W were the starting points for the geometrical calculations. In order to estimate the energetic gain due to the hydration of the S-Ket\_R-PEA salt, four different models of the (S)-ketoprofen heterochiral salt with different water occupancies (0, 1/4, 1/2, and 1) were optimized.

The HSEsol-3c was chosen for the optimization and energetics for its computationally demonstrated efficiency with an accuracy comparable to converged basis set dispersion corrected DFT.<sup>34</sup> The HSEsol-3c is based on an HSE-3c functional<sup>35</sup> extended for solid-state calculation. It is augmented with semiclassical correction potentials, and it is designed for the simulation of noncovalent interactions in large systems and for the solid state. The revised double- $\zeta$  quality atomic basis set was used.<sup>34</sup> The CRYSTAL17 software package was used for all the calculations.<sup>36</sup>

**Cambridge Structural Database Survey.** The Cambridge Structural Database (CSD, version 5.42)<sup>37</sup> was searched for crystal structures (3D coordinates determined and only organics) containing the 1-phenylethylammonium cation (Scheme 2, left) and the aromatic

Scheme 2. Molecular Fragments Searched in the CSD



carboxylate derivative fragment (Scheme 2, middle) to get information about the conformational preferences of the ammonium and carboxylate groups in these ions: 403 and 86 hits were found, respectively.

Then, structures containing both the PEA cation and the carboxylate derivative (Scheme 2 right, 3D coordinates determined, only organics) were searched; in this case, attention was paid to the H-bond motif which holds together the ions: 205 hits were found in the CSD, among which 6 pairs of diastereomeric salts were found (with the chiral  $\alpha$ -carbon, 3D coordinates determined, no -OH and -NH H-bond acceptors/donors in the carboxylate derivative, no solvent molecules) including S-Ibu\_S-PEA and S-Ibu\_R-PEA: AFINEJ/NMACEP;<sup>38</sup> COVLAC/COVLK;<sup>39</sup> IRONEJ/IRONIN;<sup>40</sup> JASJIX/QANPIF;<sup>41</sup> ODIQEZ/<sup>42</sup>YARRER.<sup>43</sup>

## RESULTS

**Procedures for Salt Preparation.** As mentioned above, the S\_Nap\_R-PEA salt has already been described under the CSD refcode HIFRIX;<sup>25</sup> however, the authors did not highlight the method used for obtaining the salt and the related single crystals. For S-Ibu\_S-PEA (CSD refcode: VAKVEK), a solventless procedure followed by methanol dissolution and slow evaporation at rt is reported,<sup>24</sup> while, according to the authors, poor-quality crystals of S-Ibu\_R-PEA (CSD refcode: VUCHOR) were obtained from ethanol.<sup>23</sup>

Considering that in the pharmaceutical industry salts are typically produced in solution, all the investigated salts were synthesized by traditional solution-based methodologies. All the syntheses were carried out by using the same solvent mixtures (ethanol/water in different ratios and amounts),

where PEA resulted as miscible. In all cases, slow solvent evaporation resulted in SCXRD-quality crystals. The salt preparation procedure was slightly modified according to the different solubilities and/or behavior of S-Ibu, S-Nap, and S-Ket in the adopted solvent mixtures (details in Supporting Information).

**Molecular Structures from Single-Crystal X-ray Diffraction.** The asymmetric unit of the anhydrous diastereomeric salts S-Ibu\_S-PEA, S-Nap\_R-PEA, S-Nap\_S-PEA, S-Ket\_S-PEA, and S-Ket\_R-PEA contains one NSAID anion and one 1-phenylethylammonium cation, while in S-Ket\_R-PEA\_W, it also includes one disordered water molecule (occupancy factor 0.15). For comparative purposes, the following discussion will also comprise the structure of S-Ibu\_R-PEA (VUCHOR, data collected at 111 K).<sup>23</sup> As for S-Ibu\_S-PEA and S-Nap\_R-PEA, lowering the temperature (100 vs 173 K and rt, respectively) does not produce any significant rearrangement of the structures, both at the molecular and crystal levels (*vide infra*).

Similarities and differences in the conformations adopted by the PEA cations in the seven salts are well illustrated in Figure 2. Table S1 in the Supporting Information lists the most

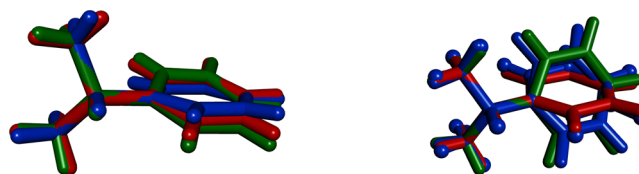
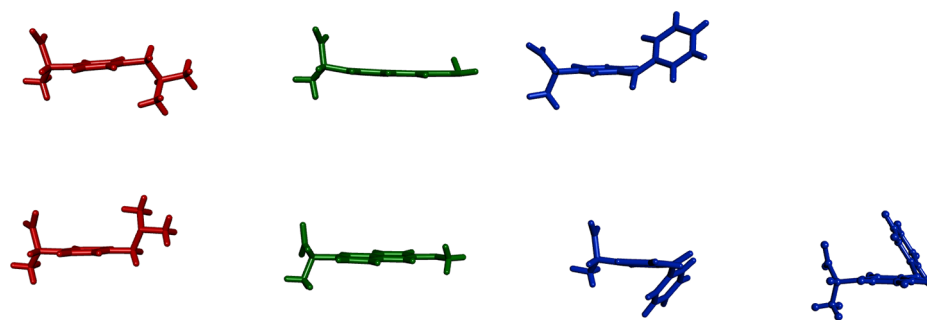


Figure 2. Superimposition of S-PEA (left) and R-PEA (right) in the salts with (S)-ibuprofen (red), (S)-naproxen (green), and (S)-ketoprofen (blue, ball and stick for the S-Ket\_R-PEA\_W salt).

significant dihedral angles which define their conformation. In the homochiral salts, the S-PEA cations are almost perfectly superimposable, while a larger conformational variability is observed in the heterochiral species (Figure 2, right). In particular, the orientation adopted by the ethylammonium moiety in the S-Nap\_R-PEA and S-Ket\_R-PEA salts appears less populated in the CSD. As for the NSAIDs, there is not a definite trend in the orientation of the propionate group depending on the overall chirality (SS versus SR) of the salts (Figure 3 and Table S1). In other words, the orientation of the propionate group does not change significantly within the series, except for S-Ibu\_R-PEA (see also Figure S21), and it is consistent with the torsional data extracted from a search in the CSD (except for the orientation observed in S-Ket\_S-PEA which is quite uncommon). Despite these similarities, the S-Ibu as well as the S-Ket anions adopt different overall shapes in their salts (see Figure 3).

In fact, on the basis of the relative orientation of the methyl and isobutyl groups, the ibuprofen molecule shows a U and a chair shape in S-Ibu\_S-PEA and S-Ibu\_R-PEA, respectively (Figure 3). On the same grounds (relative orientation of the methyl and final phenyl groups), the ketoprofen anion shows an overall U shape in S-Ket\_R-PEA, while it is chair-shaped in the S-Ket\_S-PEA and S-Ket\_R-PEA\_W salts (Figure 3).

**Crystal Structures from Single-Crystal X-ray Diffraction.** As expected,<sup>22</sup> in the salts, the NSAIDs and PEA ions are assembled through the 1-phenylethylammonium-carboxylate supramolecular heterosynthon,<sup>44</sup> which is also observed in the hydrated species of S-Ket\_R-PEA (S-Ket\_R-PEA\_W). Each



**Figure 3.** From left to right (S)-ibuprofen (red), (S)-naproxen (green), and (S)-ketoprofen (blue, stick in anhydrous, ball and stick in the hydrate salts) in the homochiral (top) and heterochiral (bottom) salts.

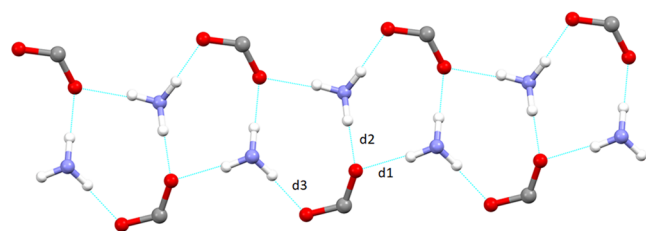
1-phenylethylammonium cation is involved in three charge-assisted  $N^+-H\cdots O^-$  hydrogen bonds<sup>45</sup> with three carboxylate groups, as already found in the crystal structures of **S-Ibu\_S-PEA** and **S-Ibu\_R-PEA** determined at 173 and 111 K, respectively (VAKVEK and VUCHOR) and in the rt structure of **S-Nap\_R-PEA** (HIFRIX). The distances separating the ammonium nitrogen and the carboxylate oxygen atoms in the seven salts are listed in Table 2. In all crystal structures a H-

**Table 2.** Distances (Å) Separating the Ammonium Nitrogen and the Carboxylate Oxygen Atoms

diastereomeric salt	$d_1$	$d_2$	$d_3$
<b>S-Ibu_S-PEA</b>	2.732(3)	2.786(3)	2.719(3)
<b>S-Ibu_R-PEA</b> <sup>a</sup>	2.764	2.695	2.812
<b>S-Nap_S-PEA</b>	2.771(3)	2.808(2)	2.663(3)
<b>S-Nap_R-PEA</b>	2.703(3)	2.871(3)	2.760(3)
<b>S-Ket_S-PEA</b>	2.724(7)	2.791(7)	2.822(6)
<b>S-Ket_R-PEA</b>	2.785(4)	2.861(4)	2.739(4)
<b>S-Ket_R-PEA_W</b>	2.757(4)	2.720(3)	2.781(4)

<sup>a</sup>See ref 23.

**Scheme 3.** Drawing of the H-Bonded Column<sup>a</sup>



<sup>a</sup>H-bonds are shown in cyan, together with the distances separating the nitrogen and oxygen atoms involved in the bond.

bonded ring originates (Scheme 3), made up of three and four H-bond acceptors and donors, respectively, which, according to graph set notation,<sup>46</sup> can be categorized as  $R_4^3(10)$ . This motif is usually present in the crystal structures containing 1-phenylethylammonium ions and carboxylate moieties, as provided by a search in the CSD. In particular, 205 hits featuring the PEA cation and the carboxylate fragment sketched in Scheme 2 (right) were found: 98 hits characterized by no -OH and -NH additional H-bond acceptor/donor groups in the monocarboxylate derivative and no cocrystallized solvent molecules were selected; 95 of them feature the  $R_4^3(10)$  H-bond motif.

The  $R_4^3(10)$  motif extends along the shortest axis direction, giving rise to a hydrogen-bonded column arranged about the two-fold screw axis (Scheme 3), referred to as a type II column.<sup>47</sup> As already noticed for the S-Ibu salts,<sup>23,24</sup> also in the anhydrous S-Ket ones the homochiral species is characterized by a shorter repeat distance (ca. 0.5 Å), while in the S-Nap salts they are comparable. Additional contacts of  $CH\cdots OOC$  type between adjacent NSAID anions as in **S-Ibu\_S-PEA** ( $C2H2\cdots O2$ , 2.42(4) Å, 155(3)°) and in **S-Ket\_R-PEA** ( $C6H6\cdots O2$ , 2.58(6) Å, 128(4)°), as well as between adjacent PEA and naproxen ions in **S-Nap\_R-PEA** ( $C2PH2PC\cdots O1$  and  $C2PH2PC\cdots O2$ , 2.51(3) Å, 161(2)° and 2.51(3) Å, 145(2)°, respectively) further stabilize each column.

In the hydrate species **S-Ket\_R-PEA\_W**, the disordered water molecule contributes to the intracolumn H-bond network ( $O1W\cdots O2$  = 2.82(2) Å;  $O1W\cdots N1P$  = 3.12(2) Å,  $O1W\cdots H1NC$  = 2.71(4) Å,  $O1W\cdots H1NC-N1P$  = 105(3)°).

Figure 4 shows the 1-D H-bonded columns in the seven salts viewed down the  $2_1$  screw axis and illustrates well the differences and similarities in the overall shape adopted by each NSAID, as well as in the relative arrangement of the NSAID/PEA ions within each column.

For example, the NSAID and PEA aromatic rings are almost perpendicularly disposed in **S-Ibu\_R-PEA** (77°), in both the naproxen salts (**S-Nap\_S-PEA**, 77°; **S-Nap\_R-PEA**, 87°), and in **S-Ket\_R-PEA** (73°) and **S-Ket\_R-PEA\_W** (86°), while they are disposed at about 50° in **S-Ibu\_S-PEA** (52°) and **S-Ket\_S-PEA** (43°).

Finally, the overall relative arrangement of the NSAID and PEA ion pairs, which is very similar in **S-Ibu\_R-PEA** and **S-Ket\_R-PEA\_W**, outlines a sort of pocket which, in the latter, hosts the crystallization water molecule (*vide infra*).

In addition, in both the ibuprofen salts, in **S-Nap\_S-PEA** and in the anhydrous and hydrate **S-Ket\_R-PEA** salts, the NSAID and PEA -CH<sub>3</sub> groups are arranged head-to-tail, while in **S-Nap\_R-PEA** and **S-Ket\_S-PEA** they are head-to-head. In the head-to-tail group of anhydrous salts, the methyl group provided by the PEA cation always points toward a facing phenyl ring provided by the H-bonded NSAID anion resulting in  $CH_3\cdots\pi$  interactions (see Table S2). In **S-Ket\_R-PEA**, further  $-CH_3\cdots\pi$  contacts are present between the methyl group provided by ketoprofen and the PEA aromatic ring (see Table S2), while in **S-Ibu\_R-PEA** a  $CH\cdots\pi$  contact involves the chiral carbon atom of the anion and the aromatic ring of the facing PEA (see Table S2). In **S-Ket\_S-PEA**, NSAID-PEA-NSAID sequences weakly interact through T-shaped  $\pi\cdots\pi$  contacts, while in **S-Nap\_R-PEA** the same kind of interaction binds NSAID-PEA pairs (see Table S2).



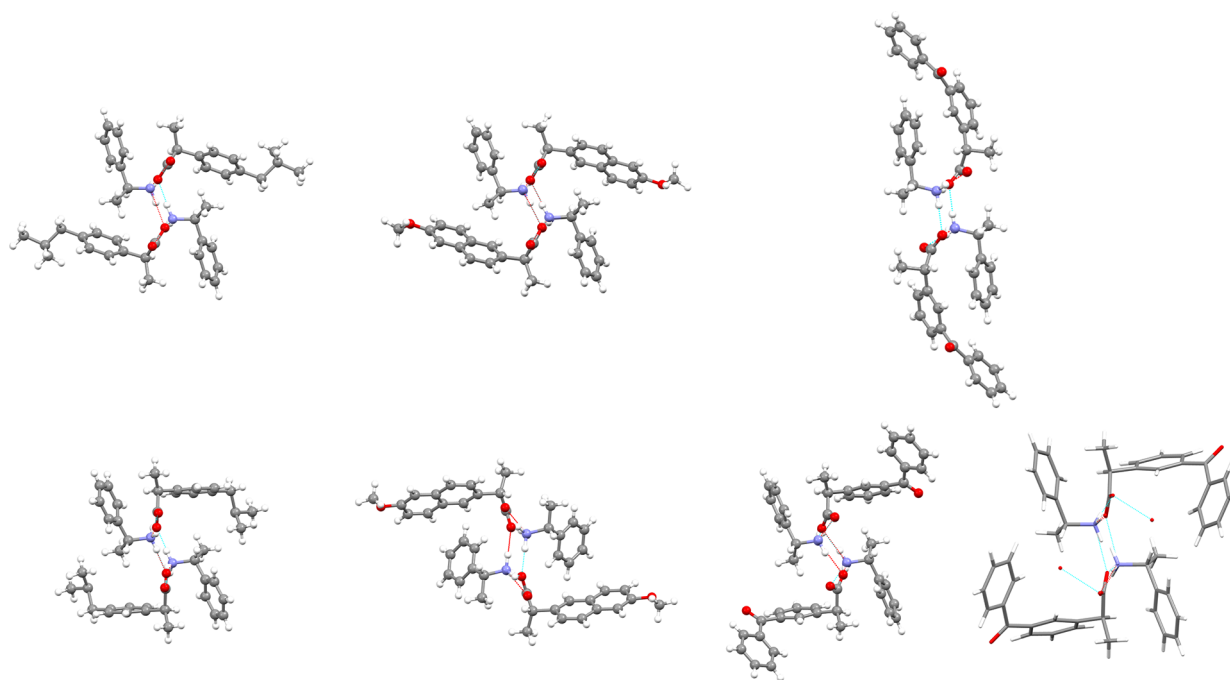


**Figure 4.** Columns viewed down the 2<sub>1</sub> axis: S-Ibu (left), S-Nap (middle), and S-Ket (right) salts with S-PEA (top) and R-PEA (bottom). S-Ket\_R-PEA\_W is represented as sticks.

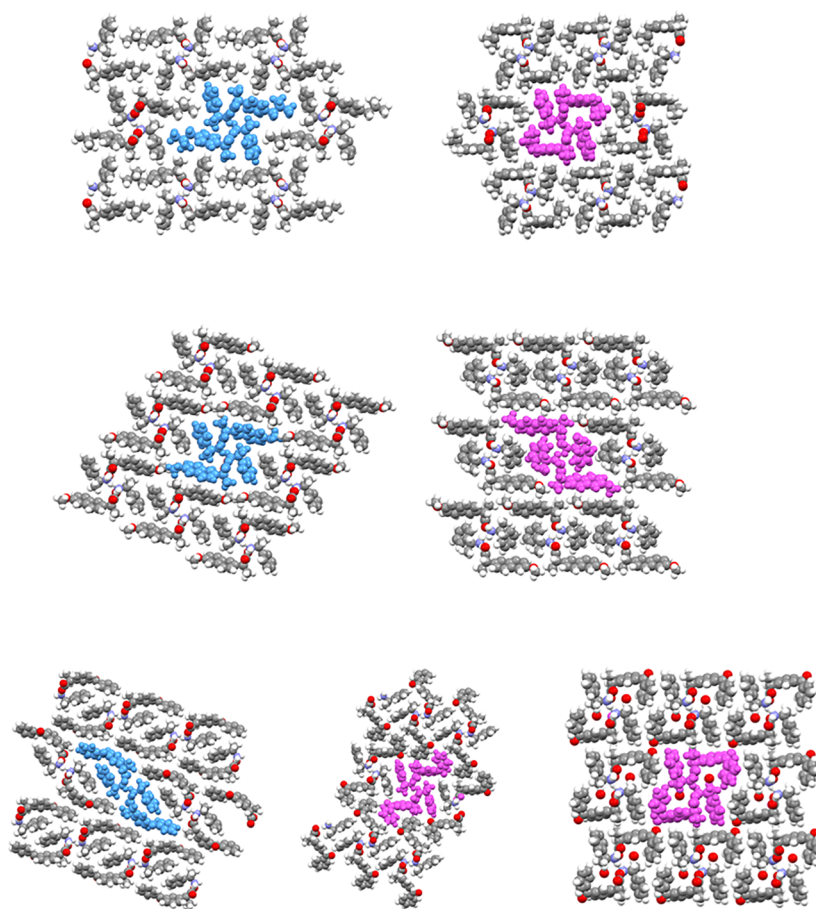


**Figure 5.** Crystal packings (viewed down the 2<sub>1</sub> axis of the column) of S-Ibu\_S-PEA (top left) and S-Ibu\_R-PEA (top right); S-Nap\_S-PEA (middle left) and S-Nap\_R-PEA (middle right); S-Ket\_S-PEA (bottom left), S-Ket\_R-PEA (bottom center), and S-Ket\_R-PEA\_W (bottom right).

Table 3. Bulk Properties Derived from SCXRD and Thermal Experiments

diastereomeric salt	SCXRD			DSC			Melting Point apparatus
	density (g/cm)	K.P.I.	T (K)	peak (K)	extrapolated peak (K)	$\Delta H$ (kJ/mol)	T (K)
S-Ibu_S-PEA	1.101	64.9	100	452.59 <sup>a</sup>	452.86 <sup>a</sup>	53.4 <sup>a</sup>	447.2–448.2
S-Ibu_R-PEA	1.085	63.8	110	430.45 <sup>a</sup>	431.00 <sup>a</sup>	41.7 <sup>a</sup>	427.5–428.2
S-Nap_S-PEA	1.216	67.8	100	446.18 <sup>a</sup>	446.60 <sup>a</sup>	50.5 <sup>a</sup>	445.0–446.0
S-Nap_R-PEA	1.263	70.5	100	415.7 <sup>b</sup> /430.2 <sup>ad</sup>	416.0 <sup>b</sup> /430.1 <sup>ad</sup>		428.7–429.5
S-Ket_S-PEA	1.229	69.1	100	402.69 <sup>a</sup>	402.84 <sup>a</sup>	29.3 <sup>a</sup>	400.2–401.1
S-Ket_R-PEA	1.225	68.2	100	395.98 <sup>a</sup>	396.47 <sup>a</sup>	37.2 <sup>a</sup>	394.0–394.9
S-Ket_R-PEA_W	1.193		100	343.42 <sup>c</sup> /394.26 <sup>a</sup>	346.2 <sup>c</sup> /394.55 <sup>a</sup>	95.0 <sup>c</sup> /–	

<sup>a</sup>Melting. <sup>b</sup>Decomposition. <sup>c</sup>Dehydration. <sup>d</sup>Melting of the S-naproxen acid.

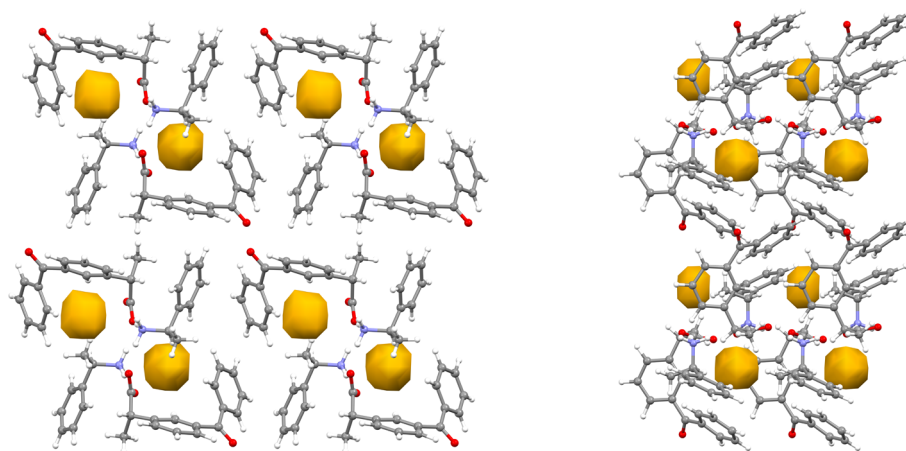


Figure 6. Crystal packing view of S-Ket\_R-PEA\_W viewed down the *b* (left) and *a* (right) axis directions showing the voids (probe radius 1.2 Å) formed upon the *in-silico* removal of the disordered water molecule.

Depending on the space group, two types of relative arrangements of the columns can be recognized: a parallel packing (columns are parallelly aligned,  $P2_1$  space group) and an antiparallel packing (columns run in alternate directions,  $P2_12_12_1$  space group).  $\text{CH}\cdots\pi$  contacts exist between the different columns, except for S-Ket\_R-PEA (see Table S3), supported by  $\text{CH}\cdots\text{OCH}_3$  and  $\text{CH}\cdots\text{O}=\text{C}$  in the naproxen and ketoprofen salts, respectively.

In both ibuprofen salts, columns are connected through ibuprofen-PEA T-shaped  $\pi\cdots\pi$  contacts (Figure 5 top). In S-Nap\_S-PEA, PEA–PEA and naproxen–naproxen T-shaped  $\pi\cdots\pi$  interactions are present, and in S-Nap\_R-PEA naproxen anions are involved in  $-\text{OCH}_3\cdots\pi$  contacts (Figure 5 middle); finally, in both salts, the methoxy oxygen atom also contributes to reinforce the crystal lattice, acting as a H-bond acceptor. In S-Ket\_S-PEA, PEA–PEA T-shaped  $\pi\cdots\pi$  interactions are present (Figure 5 bottom left). As for the heterochiral salts, in S-Ket\_R-PEA, the carbonyl oxygen atom acts as a bifurcated acceptor toward the hydrogen atoms provided by PEA and ketoprofen ions of two different columns (Figure 5 bottom center), while in S-Ket\_R-PEA\_W, ketoprofen-PEA T-shaped  $\pi\cdots\pi$  contacts as well as  $\text{CH}\cdots\text{O}=\text{C}$  interactions involving the H atoms belonging to two ketoprofen ions of the same columns are present (Figure 5, bottom right).

The most important intermolecular contacts described above are also well evidenced by the Hirshfeld surface (HS) analysis and the related fingerprint plots (details in Supporting Information; see also Figures S22–S28).

A visual comparison of the crystal packings shown in Figure 5 illustrates well the different packing efficiencies in the six anhydrous salts. The S-Ibu salts are definitely less efficiently

packed than the S-Nap and S-Ket ones, as also quantified by the crystal density and the Kitaigorodskii packing index (K.P.I.)<sup>48,49</sup> listed in Table 3, while S-Nap\_R-PEA is the most densely packed. Finally, the ibuprofen and ketoprofen homochiral salts are more efficiently packed than the corresponding heterochiral ones (Table 3), and they melt at a higher temperature (*vide infra*).

As for the hydrated species, the calculated density based on the crystallographic data is definitely lower than the corresponding anhydrous ketoprofen-PEA salt. Consistent with the low occupancy factor of the crystallization water molecule, its *in-silico* removal results in a very small fraction of empty volume (1.1%); the resulting voids show that the water molecules are lodged in isolated pockets (Figure 6).

**Variable-Temperature Analysis.** The behavior of the seven NSAID/PEA salts as the temperature changes was investigated by means of DSC, TGA, and XRD (both single crystal and powder).

First, the stability of each crystal phase in the 100 K to rt range was checked by monitoring the cell parameters at different temperatures by SCXRD (Table S4): no phase transitions occurred. Above rt, the thermal behavior of the seven salts was initially investigated putting each compound in an oven for 2 h (details in the Experimental Section), and then the resulting samples were characterized by PXRD and <sup>1</sup>H NMR, the latter to evaluate the API/PEA ratio. Data from this preliminary investigation were then compared with TGA, DSC and, in some cases, also with variable-temperature PXRD (VT-PXRD) outcomes. The results are summarized as follows.

**S-Ibuprofen Salts.** In the oven at 420 K (i.e., 30 deg below the Buchi melting point), a complete loss of S-Ibu\_S-PEA



occurred, while at a lower temperature (390 K), PXRD data (see Figure S29) showed that **S-Ibu\_S-PEA** is still present at the end of the experiment. From the NMR spectrum, a **S-Ibu/S-PEA** ratio of 8:1 can be estimated; the TGA curve consistently showed a continuous mass loss, starting at about 380 K, followed by the complete disappearance of the salt (Figure S30).

A similar result was observed for **S-Ibu\_R-PEA** (Figure S31); at 400 K, a partial decomposition of the salt, with loss of R-PEA, occurred, as evidenced by NMR (at the end of the experiment, the **S-Ibu/R-PEA** ratio was 12:1) and TGA data (see Figure S32).

The DSC curves of both **S-Ibu** salts show just one endothermic peak (50 and 30 K above the beginning of mass loss observed in the TGA, for **S-Ibu\_S-PEA** and **S-Ibu\_R-PEA**, respectively, Figures S33 and S34). This may be due to the different procedures adopted for the experiments: an almost closed pan for DSC (the lid of the aluminum pan was only punctured) versus the open one adopted in TGA (measurements were performed under an air flux of 100 mL/min), a fast DSC experiment (heating rate 10 K/min) versus 2 h in the oven.

**S-Naproxen Salts.** **S-Nap\_S-PEA** partially decomposed after 2 h at 415 K in the oven: both the salt and *S*-naproxen acid are present in the sample at the end of the experiment (as provided by the PXRD pattern of the sample, Figure S35). Consistently, a 6:1 **S-Nap/PEA** ratio was estimated from the NMR spectrum. The TGA also confirmed the salt decomposition at 420 K with a mass loss of 35.2%, which corresponds to the loss of one PEA molecule for each naproxen (Figure S36).

**S-Nap\_R-PEA** also decomposes when kept in a oven for 2 h at 400 K, but in this case the resulting sample contains only the *S*-naproxen acid as provided by the NMR data and the PXRD pattern (Figure S37). As for the TGA, the curve shows a mass loss of about 33% at about 421 K, which agrees with the loss of one PEA molecule for each naproxen (Figure S38).

VT-PXRD experiments carried out on both salts showed that during the heating steps no phase changes occurred until the complete amorphization of the samples (Figures S39 and S40).

As for **S-Nap\_S-PEA**, upon cooling, the melt did not immediately recrystallize; in the PXRD pattern collected the day after (Figure S41), only the *S*-Nap acid can be recognized (the salt did not recrystallize). As far as the heterochiral salt is concerned, upon lowering the temperature (see Figure S42) a new crystalline phase forms from the melt, which was ground after 24 h. The collected PXRD pattern evidenced (Figure S43) that the crystalline phase contains the *S*-naproxen acid.<sup>50</sup>

As already observed for the **S-Ibu/PEA** salts, in the DSC curve of **S-Nap\_S-PEA** there is just one endothermic peak at about 446 K (i.e., about 25 deg above the decomposition temperature observed during the TGA and VT-PXRD experiments, Figure S44). It is worth noting that DSC curves collected at different heating rates (5, 10, and 20 K/min) gave the same results.

Finally, for **S-Nap\_R-PEA**, two endothermic peaks were observed in the DSC curve (rt to 470 K range), compatible with the salt decomposition observed in the TGA curve and during the VT-PXRD experiment, and with the melting of the naproxen acid ( $T_m = 425$  K): peak = 415.3 K, extrapolated peak = 415.4 K and peak = 429.3 K, extrapolated peak = 429.3 K, respectively (see Figure S45).

**S-Ketoprofen Anhydrous Salts.** No decomposition/phase changes occurred in the **S-Ket\_S-PEA** and **S-Ket\_R-PEA** salts when kept in the oven for 2 h at 370 and 360 K, respectively: the PXRD patterns collected at the beginning and at the end of the experiment are well superimposable (Figures S46 and S47), and the NMR spectra of the samples at the end of the experiment gave **S-Ket/PEA** ratios of 1.5:1 and 1.2:1 for **S-Ket\_S-PEA** and **S-Ket\_R-PEA** respectively. In the DSC curves (see Figures S48 and S49), the endothermic events occurred at 403 and 396 K for **S-Ket\_S-PEA** and **S-Ket\_R-PEA**, respectively.

TGA evidenced a mass loss of about 10% at about 400 K for **S-Ket\_S-PEA** and 390 K for **S-Ket\_R-PEA** (Figures S50 and S51), suggesting partial decomposition of the salts with consequent release of the amine.

**S-Ketoprofen Hydrate Salt.** The hydrated salt, **S-Ket\_R-PEA\_W**, transformed into the anhydrous phase **S-Ket\_R-PEA** when kept in the oven for 2 h at 360 K (see Figure S52 for the PXRD patterns). Accordingly, from the NMR spectrum, a **S-Ket/PEA** ratio of 1.15:1 can be estimated. The DSC curve showed a very broad peak at about 350 K (peak = 343.42 K, extrapolated peak = 346.62 K,  $\Delta H = 95.0$  kJ/mol), which can be related to the loss of water and to the hydrate  $\rightarrow$  anhydrous transition, and a peak at about 390 K (peak = 394.26 K, extrapolated peak = 394.55 K) due to the **S-Ket\_R-PEA** melting (see Figure S53). The TGA experiment evidenced (see Figure S54) a weight loss of 1% between 313 and 373 K, which corresponds to a calculated water loss of 0.2 water molecules (consistent with the water occupancy factor as determined from the SCXRD data).

A VT-PXRD experiment performed on **S-Ket\_R-PEA\_W** confirmed the above findings: at 350 K, the unique crystalline phase present in the sample is the anhydrous **S-Ket\_R-PEA** one. At 370 K, an amorphous phase was present (Figure S55), and no recrystallization was observed when lowering the temperature. The NMR spectrum evidenced that the **S-Ket/R-PEA** ratio in the sample at the end of the experiment was 2:1, i.e., part of the R-PEA had left the melt.

The stability of the hydrate phase toward the dehydration process was also tested by putting the **S-Ket\_R-PEA\_W** in a closed chamber with KOH for a week. The PXRD patterns collected at the beginning and at the end of the experiment superimpose well on each other (Figure S56): no dehydration of the sample occurred in this experimental condition.

The reverse transformation, i.e., anhydrous  $\rightarrow$  hydrate, of the heterochiral salt occurred when the anhydrous phase **S-Ket\_R-PEA** was put in a closed chamber for a week at constant relative humidity (ca. 75%, by using a saturated solution of NaCl) as provided by the PXRD patterns (Figure S57).

It is noteworthy that, keeping the anhydrous homochiral salt (**S-Ket\_S-PEA**) in the same experimental conditions, no hydration process was observed (Figure S58).

A series of solid-state calculations were then run to shed more light onto similarities/differences in the hydrated and anhydrous heterochiral **S-Ket** salts. The anhydrous salt **S-Ket\_R-PEA-o**, the hydrated salt with full water occupancy, i.e., **S-Ket\_R-PEA\_WF-o**, and without any water molecules, **S-Ket\_R-PEA\_WE-o** were first optimized. The calculated volume of **S-Ket\_R-PEA\_WE-o** is 3% smaller than that of **S-Ket\_R-PEA\_WF-o**. In any case, a void of 17 Å<sup>3</sup> is still visible where the water solvent molecule was located for **S-Ket\_R-PEA\_WF-o**. From an energetic point of view, the stabilization

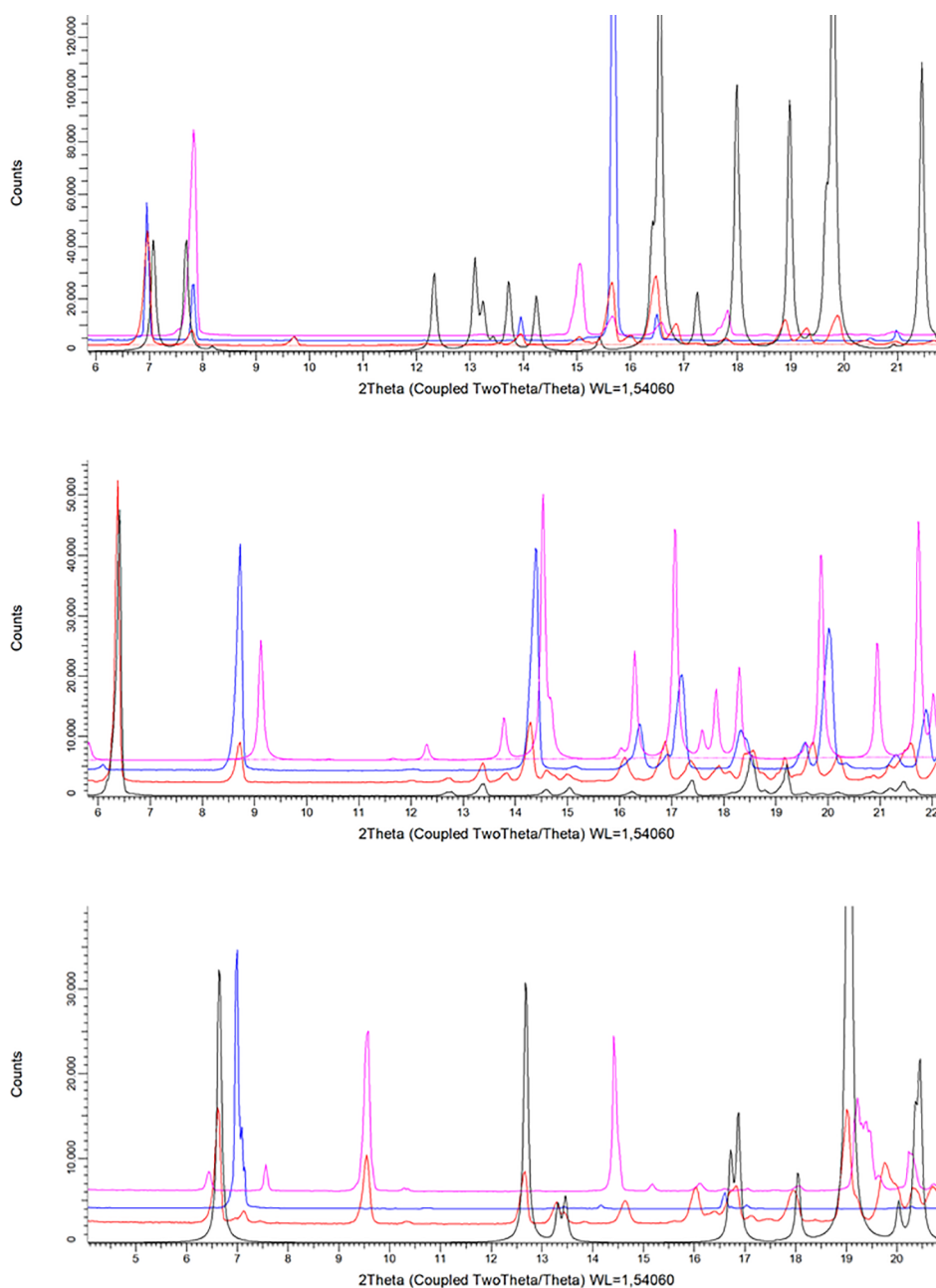


**Figure 7.** PXRD patterns. Top: S-Ibu (black), sample after 6 days in desiccator with *rac*-PEA (red), S-Ibu\_S-PEA (blue), S-Ibu\_R-PEA (magenta); middle: S-Ket (black), sample after 6 days in desiccator with *rac*-PEA (red), S-Ket\_S-PEA (blue), S-Ket\_R-PEA (magenta); bottom: S-Nap (black), sample after 6 days in desiccator with *rac*-PEA (red), S-Nap\_S-PEA (blue), S-Nap\_R-PEA (magenta).

of S-Ket\_R-PEA\_WF-o is around 75 kJ/mol, 37.4 kJ/mol for the hemihydrate salt, and it reduces to 18.4 kJ/mol for the S-Ket\_R-PEA\_W1/4-o (site occupancy for the water molecule 0.25). These data suggest that just a small occupancy as found in the experimental structure is enough for the stabilization of the S-Ket\_R-PEA\_W skeleton. On the other hand, the energy difference between the two S-Ket\_R-PEA-o and S-Ket\_R-PEA\_WE-o polymorphs is less than 0.4 kJ/mol, but S-Ket\_R-PEA-o is denser than S-Ket\_R-PEA\_WE-o (0.05 g/cm<sup>3</sup>), and S-Ket\_R-PEA-o does not show any voids in the packing. In conclusion, just a few water molecules and their hydrogen bonds are able to stabilize the packing arrangement of S-Ket\_R-PEA\_W. On the other hand, the complete removal of the water molecules in S-Ket\_R-PEA\_W starting at 313 K (TGA data) irreversibly destabilizes the dehydrated arrange-

ment of S-Ket\_R-PEA\_W, and the salt rearranges to the structure of S-Ket\_R-PEA, as shown by the variable-temperature powder X-ray diffraction experiment.

#### Preliminary Sorption Tests of *rac*-PEA on (S)-NSAIDs.

To obtain information about the ability of the NSAIDs to discriminate between the PEA enantiomers, each solid (S)-NSAID acid was kept for 6 days in a desiccator with an excess of *rac*-1-phenylethylamine (compounds were put in two different Petri dishes). Then PXRD patterns of the samples were collected.

As for S-Ibu and S-Ket, both samples contain the crystalline phases of the homochiral salts together with the corresponding free acid (Figure 7). However, in the batch containing S-Ibu, the presence of the salt containing R-PEA cannot be excluded (see in Figure 7 top the peak at  $2\theta = 21^\circ$ ). Concerning S-Nap,

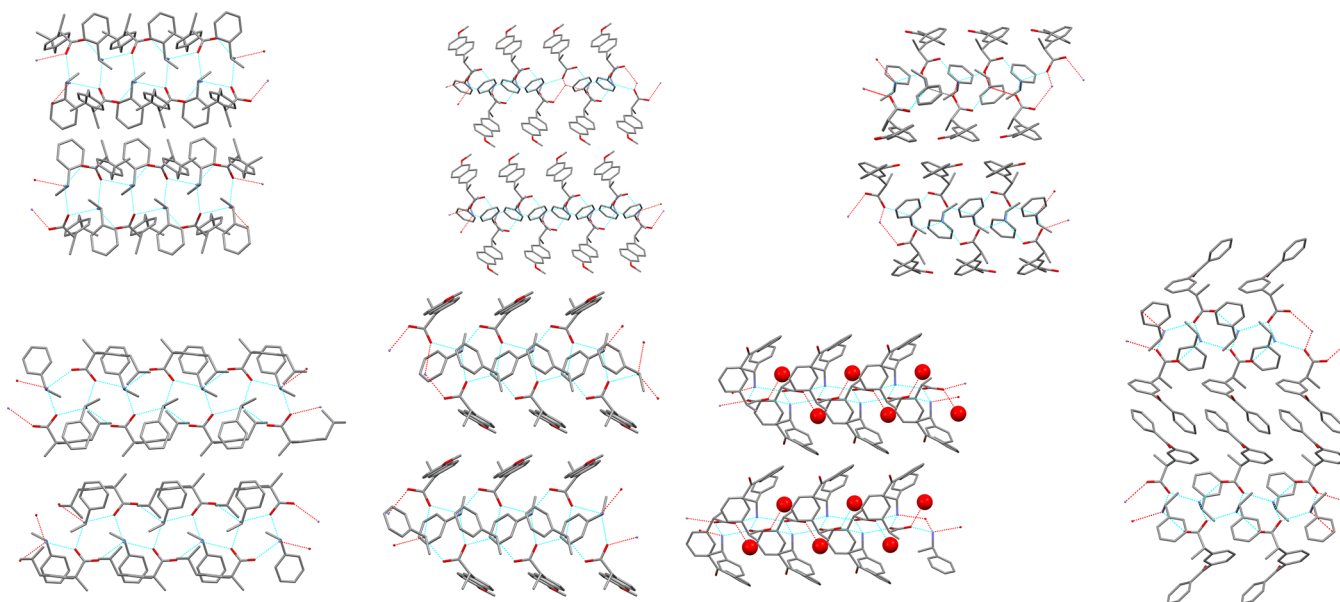


**Figure 8.** Crystal packings of left = S-Ibu\_S-PEA (top), S-Ibu\_R-PEA (down); middle = S-Nap\_S-PEA (top), S-Nap\_R-PEA (down); right = S-Ket\_S-PEA (top), S-Ket\_R-PEA\_W and S-Ket\_R-PEA (down).

at the end of the experiment the free S-Nap acid is still present together with both the homo- and heterochiral salts (see Figure 7, bottom).

## DISCUSSION

The results reported above mainly focus on two aspects: the in-depth study of the crystal packing of structurally related NSAID-PEA diastereomeric salts and of the stability/transformation of their solid forms under different experimental conditions (temperature and environment). Both kinds of investigations were carried out with the aim of extracting useful information to shed light onto the forces/features which could possibly lead to the chiral separation of their corresponding racemic compounds.

In all the investigated DSs, due to the supramolecular heterosynthon involving the 1-phenylethylammonium and the carboxylate group (which leads to the formation of the  $R_4^3(10)$  motif), columns disposed along the  $2_1$  screw axis are present. In some cases, columns are further stabilized or by additional  $\text{CH}\cdots\text{OOC}$  contacts (S-Ket\_R-PEA, S-Ibu\_S-PEA, and S-Nap\_R-PEA) or by an H-bond network which involves the water molecules (S-Ket\_R-PEA\_W).

In addition, depending on the relative arrangement of NSAID and PEA ions, weaker (based on the HS analysis, see Supporting Information)  $\text{CH}_3\cdots\pi$ ,  $\text{CH}\cdots\pi$ , and T-shaped  $\pi\cdots\pi$  contacts can also be recognized within the columns.

Finally, in anhydrous and hydrated S-Ket\_R-PEA salts, columns are interlinked through  $\text{CH}\cdots\text{O}=\text{C}$  contacts, as also evidenced in the corresponding HSs (see Supporting Information), while in the other DSs the intermolecular contacts between the  $2_1$  columns appear definitely weaker.

In order to try to rationalize the results of the preliminary sorption tests, i.e., the fact that with S-Ket only the homochiral salt forms, while S-Nap is not able to discriminate between the two PEA counterions (in the case of S-Ibu, the presence of the heterochiral salt cannot be excluded), the supramolecular sheets formed by the NSAID/PEA columns inside the crystals were further investigated. In the homochiral and the hydrated salts of S-Ket, in both the S-Nap DSs and in S-Ibu\_S-PEA,  $2_1$

sheets are characterized by almost planar boundary surfaces, i.e., planar versus uneven surfaces of the sheets<sup>51</sup> (see Figure 8). By contrast, in the S-Ibu heterochiral salt, the methyl group of ibuprofen projects out of the column, and in S-Ket\_R-PEA boundary surfaces are not present: i.e., ketoprofen anions belonging to different columns fit together like a jigsaw puzzle also thanks to  $\text{CH}\cdots\text{O}=\text{C}$  contacts (see Figure 8).

It is worth noting that, in H-bonded columnar structures of similar diastereomeric salts (like for example PEA salts with mandelic acid),<sup>51</sup> the presence of planar boundary surfaces, which favor a close packing, together with  $\text{CH}/\pi$  interactions have been recognized to strongly contribute to the stabilization of the crystal packing and have been correlated with the resolution efficiency.<sup>10</sup> In particular, for successful resolution, one diastereomeric salt should have a crystal packing consisting of stable columns stabilized by  $\text{CH}/\pi$  interactions and/or planar boundary surfaces (higher stability), while the other should not satisfy all three structural requirements (lower stability). The stability difference reflects on different solubilities resulting in high resolution efficiency.<sup>23,52</sup>

On this basis, the results from solid–vapor sorption tests, which further validate the Kinbara hypothesis,<sup>51</sup> can be rationalized: S-Ket (as well as S-Ibu) reveals a preferential capture toward the homochiral PEA (their homochiral salts are characterized by planar boundary surfaces at variance with the corresponding heterochiral ones), and S-Nap is not selective ( $2_1$  sheets of both salts are characterized by almost planar boundary surfaces).

The relative stability of each component of the diastereomeric pair was then checked under different environmental conditions. All solid forms are stable from 100 K to rt. As for the anhydrous species, the temperature stability range (*vide infra*) suggests the homochiral salt as the most stable form, having the DSs of S-Ibu the largest temperature difference. On the other hand, decomposition of the samples prevents the use of the heat of fusion for quantitative comparisons. In fact, all samples totally or partially decompose upon heating (TGA, DSC, and PXRD experiments), but S-Ket\_S-PEA and S-Ket\_R-PEA did not decompose when kept in the oven at 30 K



below their melting point; thus, in this respect they are the most stable salts of the series. The fact that the homochiral S-Ket salt is stable toward hydration, at variance with the heterochiral one, further suggests that its crystal structure is definitely more stable with respect to S-Ket\_R-PEA, consistent with planar boundary surfaces and also a higher density. The water uptake/loss implicates a significant rearrangement of the whole crystal (ketoprofen anion overall conformation and column arrangement). This is consistent with the fact that in the hydrated salt the water molecules occupy isolated voids as well as the lack of voids in the anhydrous species: the water molecules cannot easily come in/out of the crystal, and their removal, triggered by the temperature (exposure to KOH did not suffice), is accompanied by a rearrangement of the crystal. On the other hand, results from the solid-state calculations revealed that the S-Ket\_R-PEA\_W skeleton is definitely stabilized also by a small occupancy of water sites. For the anhydrous salt, S-Ket\_R-PEA-o, being more efficiently packed due to the absence of voids, is preferred with respect to the S-Ket\_R-PEA-WE form.

## CONCLUSION

In this paper, we have presented the results of a solid-state investigation of the diastereomeric salts of (S)-ibuprofen, (S)-naproxen, and (S)-ketoprofen with (R)-(+)- and (S)-(–)-1-phenylethylamine (including a partially hydrated species) by using a combination of experimental and *in-silico* tools with the aim of extracting suggestions about forces/features which could be exploited in view of the chiral separation of their racemic compounds. Attention has been paid to H-bonds and related patterns, CH $\cdots\pi$  and  $\pi\cdots\pi$  interactions, packing modes, packing efficiency/crystal density, voids type/shape, surface boundary type (XRD by both single crystal and microcrystalline powder, Hirshfeld surface analysis, solid-state calculations), as well as to thermal and phase stabilities and hydration/dehydration processes (variable-temperature powder X-ray diffraction, DSC, TGA).

All of the salts are 2<sub>1</sub>-column crystals, each column consisting of NSAID and 1-phenylthylammonium ions assembled via the 1-phenylethylammonium-carboxylate supramolecular heterosynthon which originates a H-bonded ring categorized as R<sub>4</sub><sup>2</sup>(10). Additional intracolumn CH $\cdots$ OOC contacts are present in S-Ibu\_S-PEA, S-Ket\_R-PEA and S-Nap\_R-PEA, while in the hydrated species (S-Ket\_R-PEA\_W) the water molecule also contributes to the intracolumn H-bond network. Intercolumns contacts are definitely weak except in S-Ket\_R-PEA, where C=O $\cdots$ H interactions contribute to reinforce the crystal lattice. In S-Ket\_S-PEA, S-Ket\_R-PEA\_W, and S-Ibu\_S-PEA, both the S-Nap diastereomeric salts, 2<sub>1</sub> sheets are characterized by almost planar boundary surfaces which, according to Kinbara,<sup>51</sup> favor a close packing. By contrast in S-Ibu\_R-PEA the methyl group of S-Ibu projects out of the column, and in S-Ket\_R-PEA ketoprofen anions belonging to different columns fit together like a jigsaw puzzle. The temperature stability range of the anhydrous salts (all the samples totally or partially decompose on heating) suggests the homochiral species as the most stable. The fact that the homochiral S-Ket salt did not hydrate, at variance with the heterochiral one, further confirms that its crystal structure is definitely more stable with respect to S-Ket\_R-PEA, consistent with a higher density and the presence of planar boundary surfaces. Results from the preliminary sorption tests (S-Ket and S-Ibu show a preferential capture

toward the homochiral PEA) further support the hypothesis that their homochiral salts are more stable with respect to the corresponding heterochiral ones, thus suggesting the important role played by the planar boundary surfaces in the stabilization of the homochiral diastereomeric salt crystal structures.

## ASSOCIATED CONTENT

### Supporting Information

The Supporting Information is available free of charge at <https://pubs.acs.org/doi/10.1021/acs.cgd.1c00886>.

TGA, DSC of S-Ibu\_S-PEA, S-Ibu\_R-PEA, S-Nap\_S-PEA, S-Nap\_R-PEA, S-Ket\_S-PEA, S-Ket\_R-PEA, and S-Ket\_R-PEA\_W; PXRD patterns; <sup>1</sup>H NMR spectra; views of the Hirshfeld surfaces; fingerprint plots; tables containing: torsion angles defining the overall shape of the NSAID and the PEA ions; intra- and intercolumns contacts; cell parameters; short discussion about the procedures adopted for the salt preparation/crystallization; results from the Hirshfeld Surface analysis (PDF)

### Accession Codes

CCDC 2100696–2100701 (for S-Ibu\_S-PEA, S-Nap\_S-PEA, S-Nap\_R-PEA, S-Ket\_S-PEA, S-Ket\_R-PEA and S-Ket\_R-PEA\_W) contain the supplementary crystallographic data for this paper. These data can be obtained free of charge via [www.ccdc.cam.ac.uk/data\\_request/cif](http://www.ccdc.cam.ac.uk/data_request/cif), or by emailing [data\\_request@ccdc.cam.ac.uk](mailto:data_request@ccdc.cam.ac.uk), or by contacting The Cambridge Crystallographic Data Centre, 12 Union Road, Cambridge CB2 1EZ, UK; fax: +44 1223 336033.

## AUTHOR INFORMATION

### Corresponding Author

Paola Paoli – Department of Industrial Engineering,  
University of Florence, Florence 50139, Italy; [orcid.org/0000-0002-2408-4590](https://orcid.org/0000-0002-2408-4590); Email: [paola.paoli@unifi.it](mailto:paola.paoli@unifi.it)

### Authors

Patrizia Rossi – Department of Industrial Engineering,  
University of Florence, Florence 50139, Italy; [orcid.org/0000-0002-6316-338X](https://orcid.org/0000-0002-6316-338X)

Jacopo Ceccarelli – Department of Industrial Engineering,  
University of Florence, Florence 50139, Italy; [orcid.org/0000-0002-0759-787X](https://orcid.org/0000-0002-0759-787X)

Stella Milazzo – Department of Industrial Engineering,  
University of Florence, Florence 50139, Italy

Juliana Morais Missina – Departamento de Química,  
Universidade Federal do Paraná, Centro Politécnico, 81530-900 Curitiba, Paraná, Brazil; [orcid.org/0000-0002-6226-9932](https://orcid.org/0000-0002-6226-9932)

Samuele Ciattini – Centro di Cristallografia Strutturale,  
University of Florence, Florence 50019, Italy

Andrea Ienco – Consiglio Nazionale delle Ricerche, Istituto di Chimica dei Composti OrganoMetallici (CNR-ICCOM),  
Florence 50019, Italy; [orcid.org/0000-0002-2586-4943](https://orcid.org/0000-0002-2586-4943)

Giulia Tuci – Consiglio Nazionale delle Ricerche, Istituto di Chimica dei Composti OrganoMetallici (CNR-ICCOM),  
Florence 50019, Italy; [orcid.org/0000-0002-3411-989X](https://orcid.org/0000-0002-3411-989X)

Maurizio Valleri – A. Menarini Manufacturing Logistics and Services s.r.l., Florence 50131, Italy

Maria Paola Giovannoni – NEUROFARBA, Pharmaceutical and Nutraceutical Section, University of Florence, Florence 50019, Italy; [orcid.org/0000-0003-0310-7850](https://orcid.org/0000-0003-0310-7850)

Gabriella Guerrini – NEUROFARBA, Pharmaceutical and Nutraceutical Section, University of Florence, Florence 50019, Italy; [orcid.org/0000-0001-6711-7965](https://orcid.org/0000-0001-6711-7965)

Luca Conti – Department of Chemistry “U. Schiff”, University of Florence, Florence 50019, Italy; [orcid.org/0000-0002-0402-1293](https://orcid.org/0000-0002-0402-1293)

Complete contact information is available at:  
<https://pubs.acs.org/10.1021/acs.cgd.1c00886>

## Funding

This work is supported by Fondazione Cassa di Risparmio di Firenze, Project 2018.0980.

## Notes

The authors declare no competing financial interest.

## ACKNOWLEDGMENTS

Authors thank CRIST (Centro di Cristallografia Strutturale, University of Firenze-Italy) where the single-crystal X-ray analysis as well as all the rt PXRD experiments were carried out. JMM thanks CAPES and CAPES-PrInt for the fellowships.

## ABBREVIATIONS

(R)-(+)-1-phenylethylamine, R-PEA; (S)-(–)-1-phenylethylamine, S-PEA; (S)-(+)-naproxen, S-Nap; (S)-(+)-ibuprofen, S-Ibu; (S)-(+)-ketoprofen, S-Ket; DS, diastereomeric salt; XRD, X-ray diffraction; SCXRD, single-crystal X-ray diffraction; PXRD, powder X-ray diffraction; VT-XRD, variable-temperature X-ray diffraction; DSC, differential scanning calorimetry; TGA, thermogravimetric analysis

## REFERENCES

- (1) Mehta, M. *Biopharmaceutics Classification System (BCS): Development, Implementation, and Growth*; Wiley, 2016.
- (2) Landoni, F.; Soraci, A. Pharmacology of chiral compounds: 2-arylpropionic acid derivatives. *Curr. Drug Metab.* **2001**, *2*, 37–51.
- (3) Nguyen, L. A.; He, H.; Pham-Huy, C. Chiral drugs: an overview. *Int. J. Biomed. Sci.* **2006**, *2*, 85–100.
- (4) Agranat, I.; Marom, H. In defense of secondary pharmaceutical patents in drug discovery and development. *ACS Med. Chem. Lett.* **2020**, *11*, 91–98.
- (5) Calcaterra, A.; D’Acquarica, I. The market of chiral drugs: Chiral switches versus de novo enantiomerically pure compounds. *J. Pharm. Biomed. Anal.* **2018**, *147*, 323–340.
- (6) Agranat, I.; Caner, H.; Caldwell, J. Putting chirality to work: the strategy of chiral switches. *Nat. Rev. Drug Discovery* **2002**, *1*, 753–768.
- (7) Foster, R. T.; Jamali, F.; Russell, A. S.; Alballa, S. R. Pharmacokinetics of ketoprofen enantiomers in healthy subjects following single and multiple doses. *J. Pharm. Sci.* **1988**, *77*, 70–73.
- (8) Mane, S. Racemic drug resolution: a comprehensive guide. *Anal. Methods* **2016**, *8*, 7567–7586.
- (9) CRC Handbook of Optical Resolutions via Diastereomeric Salt Formation; Kozma, D., Ed.; CRC Press, 2001.
- (10) Chirality in Drug Research; Francotte, E.; Lindner, W., Eds.; Wiley-VCH Verlag GmbH & Co, KGaA: Weinheim, 2006; pp 127–154.
- (11) Rossi, P.; Paoli, P.; Chelazzi, L.; Conti, L.; Bencini, A. The solid-state structure of the  $\beta$ -blocker metoprolol: a combined experimental and in silico investigation. *Acta Crystallogr., Sect. C: Struct. Chem.* **2019**, *C75*, 87–96.
- (12) Rossi, P.; Paoli, P.; Milazzo, S.; Chelazzi, L.; Ienco, A.; Conti, L. Investigating differences and similarities between betaxolol polymorphs. *Crystals* **2019**, *9*, 509–521.
- (13) Paoli, P.; Rossi, P.; Macedi, E.; Ienco, A.; Chelazzi, L.; Bartolucci, G. L.; Bruni, B. Similar but Different: The Case of

Metoprolol Tartrate and Succinate Salts. *Cryst. Growth Des.* **2016**, *16*, 789–799.

(14) Rossi, P.; Paoli, P.; Chelazzi, L.; Conti, L.; Bencini, A. Metoprolol Fumarate: Crystal Structure from Powder X-ray Diffraction Data and Comparison with the Tartrate and Succinate Salts. *Cryst. Growth Des.* **2018**, *18*, 7015–7026.

(15) Rossi, P.; Macedi, E.; Paoli, P.; Bernazzani, L.; Carignani, E.; Borsacchi, S.; Geppi, M. A. Solid-solid transition between hydrated racemic compound and anhydrous conglomerate in Na-ibuprofen: A combined X-ray diffraction, solid-state NMR, calorimetric, and computational study. *Cryst. Growth Des.* **2014**, *14*, 2441–2452.

(16) Morais Missina, J.; Conti, L.; Rossi, P.; Ienco, A.; Gioppo Nunes, G.; Valtancoli, B.; Chelazzi, L.; Paoli, P. Ibuprofen as linker for calcium(II) in a 1D-coordination polymer: A solid state investigation complemented with solution studies. *Inorg. Chim. Acta* **2021**, *S23*, 120319–120320.

(17) Paoli, P.; Rossi, P.; Chelazzi, L.; Altamura, M.; Fedi, V.; Giannotti, D. Solid State Investigation and Characterization of a Nepadutant Precursor: Polymorphic and Pseudopolymorphic Forms of MEN11282. *Cryst. Growth Des.* **2016**, *16*, 5294–5304.

(18) Paoli, P.; Milazzo, S.; Rossi, P.; Ienco, A. Rationalization of Lattice Thermal Expansion for Beta-Blocker Organic Crystals. *Crystals* **2020**, *10*, 350–360.

(19) Rossi, P.; Paoli, P.; Milazzo, S.; Chelazzi, L.; Giovannoni, M. P.; Guerrini, G.; Ienco, A.; Valleri, M.; Conti, L. A combined crystallographic and computational study on dexketoprofen trometamol dihydrate salt. *Crystals* **2020**, *10*, 659–672.

(20) Rossi, P.; Paoli, P.; Chelazzi, L.; Milazzo, S.; Biagi, D.; Valleri, M.; Ienco, A.; Valtancoli, B.; Conti, L. Relationships between Anhydrous and Solvated Species of Dexketoprofen Trometamol: A Solid-State Point of View. *Cryst. Growth Des.* **2020**, *20*, 226–236.

(21) Rossi, P.; Paoli, P.; Ienco, A.; Biagi, D.; Valleri, M.; Conti, L. A new crystal form of the NSAID dexketoprofen. *Acta Crystallogr., Sect. C: Struct. Chem.* **2019**, *75*, 783–792.

(22) Kinbara, K.; Hashimoto, Y.; Sukegawa, M.; Nohira, H.; Saigo, K. Crystal Structures of the Salts of Chiral Primary Amines with Achiral Carboxylic Acids: Recognition of the Commonly-Occurring Supramolecular Assemblies of Hydrogen-Bond Networks and Their Role in the Formation of Conglomerate. *J. Am. Chem. Soc.* **1996**, *118*, 3441–3449.

(23) Molnar, P.; Bombicz, P.; Varga, C.; Bereczki, L.; Szekely, E.; Pokol, G.; Fogassy, E.; Simandi, B. Influence of benzylamine on the resolution of Ibuprofen with (+)-(R)-phenylethylamine via supercritical fluid extraction. *Chirality* **2009**, *21*, 628–636.

(24) Lemmerer, A.; Bourne, S. A.; Caira, M. R.; Cotton, J.; Hendricks, U.; Peinke, L. C.; Trollope, L. Incorporating active pharmaceutical ingredients into a molecular salt using a chiral counterion. *CrystEngComm* **2010**, *12*, 3634–3641.

(25) Dupont, L.; Pirotte, B.; De Tullio, P.; Delarge, J. Absolute configuration of (R)-1-phenylethylammonium (S)-2-(6-methoxy-2-naphthyl)propionate. *Acta Crystallogr., Sect. C: Cryst. Struct. Commun.* **1996**, *S2*, 393–395.

(26) Bruker APEX2; Bruker AXS Inc.: Madison, Wisconsin, USA, 2012.

(27) Bruker SAINT; Bruker AXS Inc.: Madison, Wisconsin, USA, 2012.

(28) Burla, M. C.; Caliendo, R.; Camalli, M.; Carrozzini, B.; Cascarano, G. L.; De Caro, L.; Giacovazzo, C.; Polidori, G.; Spagna, R. Crystal structure determination and refinement via SIR2014. *J. Appl. Crystallogr.* **2005**, *38*, 381–388.

(29) Sheldrick, G. M. Crystal structure refinement with SHELXL. *Acta Crystallogr., Sect. C: Struct. Chem.* **2015**, *71*, 3–8.

(30) Several crystals of S-Ket\_R-PEA\_W were tested, and in all cases the occupancy factor of the oxygen atom of the water molecule converged to 0.15.

(31) STARe, Thermal Analysis Software; Mettler - Toledo Int. Inc.: Schwerzenbach, Switzerland.

(32) Macrae, C. F.; Bruno, I. J.; Chisholm, J. A.; Edgington, P. R.; McCabe, P.; Pidcock, E.; Rodriguez-Monge, E.; Taylor, R.; van de

Streek, J.; Wood, P. A. New Features for the Visualization and Investigation of Crystal Structures. *J. Appl. Crystallogr.* **2008**, *41*, 466–470.

(33) Turner, M. J.; McKinnon, J. J.; Wolff, S. K.; Grimwood, D. J.; Spackman, P. R.; Jayatilaka, D.; Spackman, M. A. *Crystal Explorer17*; University of Western Australia, 2017.

(34) Doná, L.; Brandenburg, J. G.; Civalieri, B. Extending and Assessing Composite Electronic Structure Methods to the Solid State. *J. Chem. Phys.* **2019**, *151*, 121101.

(35) Brandenburg, J. G.; Caldeweyher, E.; Grimme, S. Screened Exchange Hybrid Density Functional for Accurate and Efficient Structures and Interaction Energies. *Phys. Chem. Chem. Phys.* **2016**, *18* (23), 15519–15523.

(36) Dovesi, R.; Erba, A.; Orlando, R.; Zicovich-Wilson, C. M.; Civalieri, B.; Maschio, L.; Rérat, M.; Casassa, S.; Baima, J.; Salustro, S.; Kirtman, B. Quantum-Mechanical Condensed Matter Simulations with CRYSTAL. *Wiley Interdiscip. Rev.: Comput. Mol. Sci.* **2018**, *8* (4), e1360.

(37) Groom, C. R.; Bruno, I. J.; Lightfoot, M. P.; Ward, S. C. The Cambridge Structural Database. *Acta Crystallogr., Sect. B: Struct. Sci., Cryst. Eng. Mater.* **2016**, *B72*, 171–179.

(38) Karamertzanis, P. G.; Anandamanoharan, P. R.; Fernandes, P.; Cains, P. W.; Vickers, M.; Tocher, D. A.; Florence, A. J.; Price, S. L. Toward the Computational Design of Diastereomeric Resolving Agents: An Experimental and Computational Study of 1-Phenylethylammonium-2-phenylacetate Derivatives. *J. Phys. Chem. B* **2007**, *111*, 5326–5336.

(39) Bathori, N. B.; Nassimbeni, L. R.; van de Streek, J. One hydrogen bond does not a separation make, or does it? Resolution of amines by diacetoneketogulononic acid. *Chem. Commun.* **2015**, *51*, 5664–5667.

(40) Ichikawa, A.; Ono, H.; Echigo, T.; Mikata, Y. Crystal structures and chiral recognition of the diastereomeric salts prepared from 2-methoxy-2-(2-(1-naphthyl)propanoic acid. *CrystEngComm* **2011**, *13*, 4536–4548.

(41) Marchini, N.; Bombieri, G.; Artali, R.; Bolchi, C.; Pallavicini, M.; Valoti, E. Influence of (S)-1-phenylethylamine para substitution on the resolution of (±)-1,4-benzodioxane-2-carboxylic acid: a crystallographic, theoretical and morphologic approach. *Tetrahedron: Asymmetry* **2005**, *16*, 2099–2106.

(42) Ichikawa, A.; Ono, H.; Mikata, Y. Crystal structures of Mosher's salt and ester elucidated by X-ray crystallography. *CrystEngComm* **2013**, *15*, 8088–8096.

(43) Ichikawa, A.; Ono, H.; Mikata, Y. The crystal structure of the more-soluble Mosher's salt. *Chem. Lett.* **2017**, *46*, 550–553.

(44) Bis, J. A.; Zaworotko, M. J. The 2-aminopyridinium-carboxylate supramolecular heterosynthon: a robust motif for generation of multiple-component crystals. *Cryst. Growth Des.* **2005**, *5*, 1169–1179.

(45) Gilli, P.; Bertolasi, V.; Ferretti, V.; Gilli, G. Evidence for Intramolecular N–H···O Resonance-Assisted Hydrogen Bonding in  $\beta$ -Enaminones and Related Heterodienes. A Combined Crystal-Structural, IR and NMR Spectroscopic, and Quantum-Mechanical Investigation. *J. Am. Chem. Soc.* **1994**, *116*, 909–915.

(46) Etter, M. C.; MacDonald, J. C.; Bernstein, J. Graph-set analysis of hydrogen-bond patterns in organic crystals. *Acta Crystallogr., Sect. B: Struct. Sci.* **1990**, *46*, 256–262.

(47) Nagahama, S.; Inoue, K.; Sada, K.; Miyata, M.; Matsumoto, A. Two-Dimensional Hydrogen Bond Networks Supported by CH/ $\pi$  Interaction Leading to a Molecular Packing Appropriate for Topochemical Polymerization of 1,3-Diene Monomers. *Cryst. Growth Des.* **2003**, *3*, 247–256.

(48) Kitaigorodskii, A. I. *Organic Chemical Crystallography*; Consultants Bureau: New York, 1961; pp 106–110.

(49) Spek, A. L. *PLATON, A Multipurpose Crystallographic Tool*; Utrecht University: Utrecht, The Netherlands, 1998.

(50) CSD Refcode: COYRUD; compound: (+)-2-(6-Methoxy-2-naphthyl)-propionic acid; Ravikumar, K.; Rajan, S. S.; Pattabhi, V.; Gabe, E. J. Structure of naproxen, C<sub>14</sub>H<sub>14</sub>O<sub>3</sub>. *Acta Crystallogr., Sect. C: Cryst. Struct. Commun.* **1985**, *41*, 280–282.

(51) Kinbara, K.; Sakai, K.; Hashimoto, Y.; Nohira, H.; Saigo, K. Chiral discrimination upon crystallisation of the diastereomeric salts of 1-arylethylamines with mandelic acid or p-methoxymandelic acid: interpretation of the resolution efficiencies on the basis of the crystal structures. *J. Chem. Soc., Perkin Trans. 2* **1996**, 2615–2622.

(52) Martin, S. J.; Dale, S. M. Process for the manufacture of racemic 2-aryl-propionic acid, International patent WO2010/001103A1, January 7, 2010.